AUTHOR QUERY FORM

Journal: CELL

Article Number: 7681

Dear Author,

Please check your proof carefully and mark all corrections at the appropriate place in the proof.

Location in article	Query / Remark: Click on the Q link to find the query's location in text Please insert your reply or correction at the corresponding line in the proof
	There are no queries in this article

Thank you for your assistance.

Please cite this article in press as: Masri et al., Partitioning Circadian Transcription by SIRT6 Leads to Segregated Control of Cellular Metabolism, Cell (2014), http://dx.doi.org/10.1016/j.cell.2014.06.050

Cell

Partitioning Circadian Transcription by SIRT6 Leads to Segregated Control of Cellular Metabolism

Selma Masri,[1,2] Paul Rigor,[3,4] Marlene Cervantes,[1,2] Nicholas Ceglia,[3,4] Carlos Sebastian,[5] Cuiying Xiao,[6] Manuel Roqueta-Rivera,[7] Chuxia Deng,[6] Timothy F. Osborne,[7] Raul Mostoslavsky,[5] Pierre Baldi,[1,2,3,4] and Paolo Sassone-Corsi[1,2,4,*]

[1]Center for Epigenetics and Metabolism
[2]Department of Biological Chemistry
[3]Department of Computer Science
[4]Institute for Genomics and Bioinformatics
University of California, Irvine, Irvine, CA 92697, USA
[5]The Massachusetts General Hospital Cancer Center, Harvard Medical School, Boston, MA 02114, USA
[6]Genetics of Development and Diseases Branch, NIDDK, National Institutes of Health, Bethesda, MD 20892, USA
[7]Metabolic Disease Program, Sanford-Burnham Medical Research Institute, Orlando, FL 32827, USA
*Correspondence: psc@uci.edu
http://dx.doi.org/10.1016/j.cell.2014.06.050

SUMMARY

Circadian rhythms are intimately linked to cellular metabolism. Specifically, the NAD$^+$-dependent deacetylase SIRT1, the founding member of the sirtuin family, contributes to clock function. Whereas SIRT1 exhibits diversity in deacetylation targets and subcellular localization, SIRT6 is the only constitutively chromatin-associated sirtuin and is prominently present at transcriptionally active genomic loci. Comparison of the hepatic circadian transcriptomes reveals that SIRT6 and SIRT1 separately control transcriptional specificity and therefore define distinctly partitioned classes of circadian genes. SIRT6 interacts with CLOCK:BMAL1 and, differently from SIRT1, governs their chromatin recruitment to circadian gene promoters. Moreover, SIRT6 controls circadian chromatin recruitment of SREBP-1, resulting in the cyclic regulation of genes implicated in fatty acid and cholesterol metabolism. This mechanism parallels a phenotypic disruption in fatty acid metabolism in SIRT6 null mice as revealed by circadian metabolome analyses. Thus, genomic partitioning by two independent sirtuins contributes to differential control of circadian metabolism.

INTRODUCTION

The circadian clock regulates a host of physiological events required for energy balance (Feng and Lazar, 2012; Sahar and Sassone-Corsi, 2012; Wijnen and Young, 2006). These events provide remarkable plasticity for the organism to adapt to surrounding environmental changes, especially given the dynamic input of cellular metabolism on chromatin modifications (Gut and Verdin, 2013; Katada et al., 2012). A functional link between the circadian clock and cellular metabolism was revealed by reports implicating the SIRT1 deacetylase in clock function (Asher et al., 2008; Chang and Guarente, 2013; Nakahata et al., 2008). Mammalian sirtuins constitute a family of seven NAD$^+$-dependent deacetylases (SIRT1–7) that vary in potency of enzymatic activity and protein targets (Chang and Guarente, 2014; Hall et al., 2013; Houtkooper et al., 2012). The subcellular localization of the sirtuins varies from cytoplasm, mitochondria, nucleus, and nucleolus (Finkel et al., 2009).

Of the sirtuins, SIRT6 is unique in its constitutive localization to chromatin (Mostoslavsky et al., 2006; Tennen et al., 2010), and its genome-wide occupancy is prominent at transcriptional start sites (TSSs) of active genomic loci, which coincides to serine 5 phosphorylated RNA polymerase II binding sites (Ram et al., 2011). SIRT6 has also been reported to be dynamic in its chromatin binding in response to stimuli such as (TNFα), resulting in altering the transcriptional landscape of aging and stress-related genes (Kawahara et al., 2011). SIRT6 deacetylates H3 lysine 9 (H3K9) (Kawahara et al., 2009; Michishita et al., 2008) and H3K56 (Michishita et al., 2009; Toiber et al., 2013; Yang et al., 2009), resulting in modulation of gene expression, telomere maintenance, and genomic stability (Tennen and Chua, 2011), and the HDAC activity of SIRT6 has been found to be nucleosome dependent (Gil et al., 2013). Importantly, SIRT6 is also heavily implicated in metabolic regulation, as *Sirt6*$^{-/-}$ mice die at 2–4 weeks of age due to severe accelerated aging and hypoglycemia as a result of altered rates of glycolysis, glucose uptake, and mitochondrial respiration (Mostoslavsky et al., 2006; Xiao et al., 2010; Zhong et al., 2010). SIRT6 also controls the acetylation state of PGC-1α in a GCN5-dependent manner that regulates blood glucose levels (Dominy et al., 2012). Liver-specific *Sirt6*$^{-/-}$ mice develop fatty liver due to altered expression of genes involved in fatty acid beta oxidation and triglyceride synthesis (Kim et al., 2010).

The circadian transcriptome is thought to comprise at least 10% of all transcripts in a given tissue, though genes can gain rhythmicity depending on a tissue-specific permissive environment (Masri and Sassone-Corsi, 2010). Moreover, the potential for a specific gene to become circadian may be related to changes in the metabolic, nutritional, and epigenetic state (Eckel-Mahan et al., 2013). A number of studies have revealed the role of chromatin remodeling in providing permissive genomic organization for circadian transcription (Belden et al., 2011; DiTacchio et al., 2011; Doi et al., 2006; Duong et al., 2011; Etchegaray et al., 2003; Katada and Sassone-Corsi, 2010; Koike et al., 2012; Ripperger and Schibler, 2006). We report that SIRT6 defines the circadian oscillation of a distinct group of hepatic genes, different from the ones under SIRT1 control. This partitioning of the circadian genome is achieved by controlling the recruitment to chromatin of the core circadian activators CLOCK:BMAL1, as well as SREBP-1. The sirtuin-dependent partitioning of circadian transcription leads to differential control of hepatic lipid metabolism related to fatty-acid-dependent pathways.

RESULTS

Partitioning of the Circadian Transcriptome by SIRT6 and SIRT1 in Exclusive Subdomains

Given the unique ability of SIRT6 to function as an HDAC (Kawahara et al., 2009; Michishita et al., 2008) and transcriptional facilitator at chromatin (Kawahara et al., 2011; Ram et al., 2011), we investigated its role in controlling hepatic circadian gene expression and metabolism. DNA microarrays were used to delineate the control of SIRT6 versus SIRT1 on the circadian genome. To do so, we used mice with liver-specific ablation of either *Sirt1* or *Sirt6* genes and their corresponding wild-type (WT) littermates. Livers were harvested every 4 hr over the circadian cycle, representing zeitgeber times (ZT) 0, 4, 8, 12, 16, and 20. Groups of genes were selected based on the following criteria: group 1 represents genes that oscillate in WT (SIRT6) liver and whose oscillation is dampened/disrupted in SIRT6-deficient mice (SIRT6 KO). Group 2 represents genes that oscillate in SIRT6 KO, but not in their corresponding WT littermates. Group 3 represents genes that oscillate in WT (SIRT1) liver and whose oscillation is dampened/disrupted in SIRT1 knockout (KO) mice (SIRT1 KO). Group 4 respresents genes that oscillate in SIRT1 KO, but not in their corresponding WT littermates. The group referred to as "both" includes genes that oscillate similarly in both WT and KO groups for either SIRT6 or SIRT1 data sets. Oscillating genes were selected based on a 0.01 p value cutoff. A comparison of both WT strains can be found in Figure S1 (available online). Of the SIRT6 transcriptome, 691 genes were identified in the WT group 1, with 779 genes oscillating more robustly in the SIRT6 KO group 2 and 506 genes oscillating similarly in both groups (Figure 1A). Using the same criteria for the SIRT1 transcriptome, 703 genes oscillate in the WT group 3, with 1,126 genes oscillating with greater amplitude in the SIRT1 KO group 4 and 1,091 genes oscillating similarly in both groups (Figure 1B). This analysis revealed that, of the 1,976 rhythmic genes identified in the SIRT6 transcriptome, the expression profile of 1,470 genes was altered by SIRT6 disruption (74%). In addition, of the 2,920 oscillating genes identified in the SIRT1 experiment, 1,829 genes were changed by SIRT1 disruption (63%). Thus, SIRT6, in addition to SIRT1, significantly regulates the expression of clock-controlled genes (CCGs).

Gene ontology (GO) analysis of genes with altered circadian oscillation in SIRT6 versus SIRT1 transcriptomes revealed some striking differences (Figures 1C, 1D, and S2). The most highly represented biological processes are transcription, transcriptional regulation, and nuclear processes, enriched in both WT liver groups and SIRT1 KO livers but completely absent from the SIRT6 KO livers. In addition to transcription, enrichment in mitochondrial and intracellular non-membrane-bound organelle (GO term describing ribosomes, cytoskeleton, and chromosomes) was highly enriched. The SIRT6 KO group shared little homology with WT or SIRT1 KO groups in significantly selected biological pathways. GO terms enriched in SIRT6 KO were endoplasmic reticulum, Golgi apparatus, protein localization/catabolism, RNA processing, and translation (Figure 1C). GO biological pathway analysis highlighted unique classes of genes represented exclusively in the SIRT6 KO group, indicating that disruption of hepatic SIRT6 results in altered circadian biological function.

Next, we focused on understanding how these two sirtuins differentially regulate distinct classes of circadian genes. Importantly, there is little overlap between the groups of SIRT1- and SIRT6-dependent circadian genes (160 common genes) (Figure 2A). These are mostly implicated in cytoplasmic and mitochondrial pathways and are linked to metabolic processes and stress response, as described by GO biological pathway analysis (Figure 2A). Thus, SIRT6 and SIRT1 regulate distinct biological classes of circadian genes. For a detailed view of these genes controlled by SIRT6 or SIRT1, refer to CircadiOmics (http://circadiomics.igb.uci.edu) (Patel et al., 2012). Analysis of the circadian phase of gene expression reveals a peak in phase of the genes oscillating in SIRT6 KO mice at ZT 16 and ZT20, differently from the genes significantly expressed in SIRT1 KO mice peaking at ZT 4 and ZT8 (Figure 2B).

Circadian expression was confirmed for distinct classes of genes based on their rhythmic profile: (1) genes whose expression profile is unaltered between WT versus SIRT6 KO and SIRT1 KO. Briefly, these genes are involved in transcription and regulation of rhythmic processes, as the bulk of core clock genes are generally resistant to change in expression (Figure S2). (2) Genes whose circadian expression is similarly regulated by SIRT6 and SIRT1. Examples include *Nephronectin* (*Npnt*), encoding an extracellular matrix protein, which oscillates in WT liver and is dampened similarly in both SIRT6 KO and SIRT1 KO mice (Figure 2C). Conversely, circadian expression of *Dbp* is equally increased in amplitude at ZT 8 in both SIRT6 KO and SIRT1 KO animals (Figure 2D). These genes, although responding in opposite manner to the ablation of either sirtuin, belong to the same class of genes similarly regulated by both sirtuins. (3) Genes whose amplitude in oscillation is more robust when either SIRT6 or SIRT1 is ablated. For example, fatty acid synthase (*Fasn*), 3-hydroxy-3-methyl-glutaryl-CoA reductase (*Hmgcr*), and lanosterol synthase (*Lss*) were uniquely regulated by SIRT6, as the amplitude of circadian oscillation was enhanced in SIRT6 KO (Figure 2E). The circadian profiles of these genes

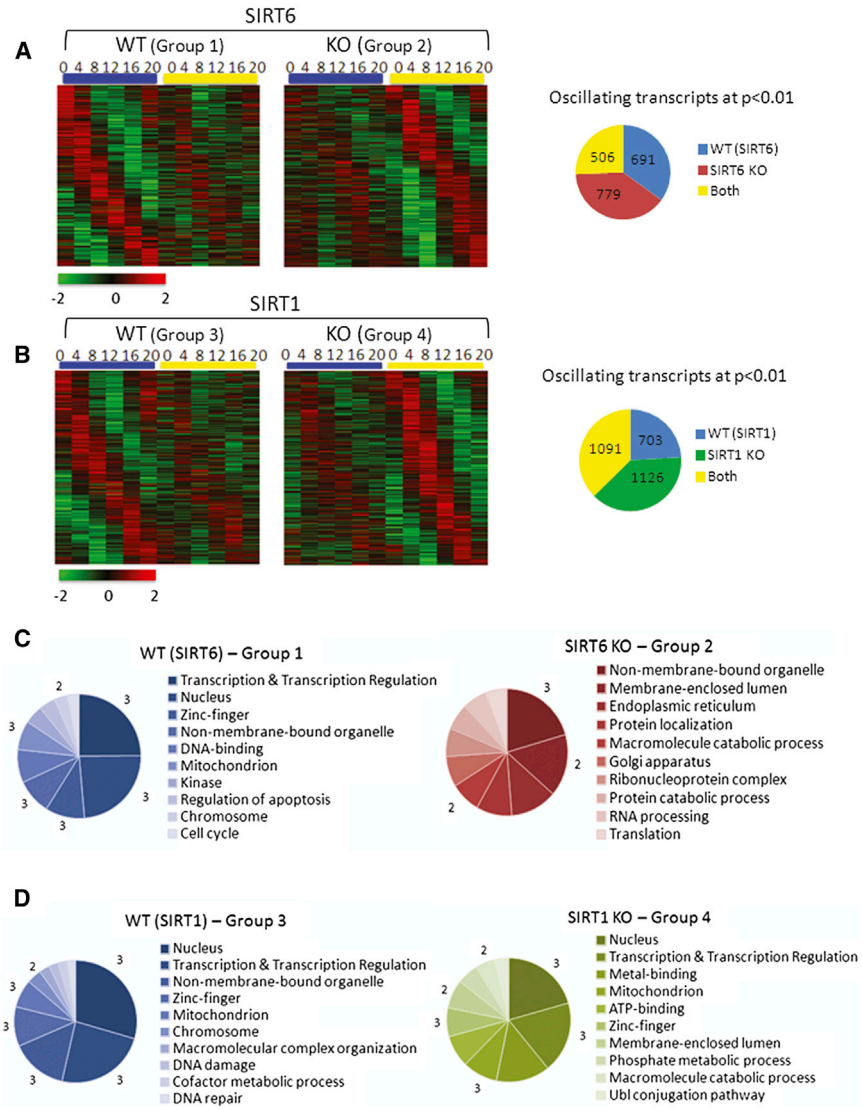

Figure 1. The SIRT6 and SIRT1 Circadian Transcriptomes

(A and B) DNA microarray analysis was performed using mouse liver total RNA from ZT 0, 4, 8, 12, 16, and 20. Using JTK_cycle, genes selected to be circadian at a p value < 0.01 are displayed as heat maps for WT and SIRT6 KO livers (A) and WT and SIRT1 KO livers (B). Heat maps on the left side show genes that oscillate in WT (groups 1 and 3) with dampened or flat gene expression in SIRT6 KO (group 2) or SIRT1 KO (group 4). Heat maps on the right side display genes with more robust circadian expression when the sirtuins are disrupted. Pie charts indicate actual numbers of circadian genes for the SIRT6 and SIRT1 transcriptomes. Biological function analysis was performed using DAVID. GO terms for molecular function, biological process, and cellular component were used.

(C and D) Top ten GO terms, based on a 0.01 p value cutoff, are shown for the SIRT6 transcriptome (C) and the SIRT1 transcriptome (D). Numbers bordering different pie slices indicate how many times that GO term was found in the four pie charts shown.

were unaltered in SIRT1 KO, as compared to WT (Figure S3A). Conversely, genes with enhanced circadian amplitude exclusively in SIRT1 KO, including regulator of G protein signaling 16 (*Rgs16*), serine dehydratase (*Sds*), and methylenetetrahydrofolate dehydrogenase 1-like (*Mthfd1l*), are shown (Figure 2F). The profiles of *Rgs16*, *Sds*, and *Mthfd1l* genes are not altered in amplitude between WT and SIRT6 KO mice (Figure S3B). Also, the expression of *Sirt6* and *Sirt1* is not altered in the SIRT1 KO and SIRT6 KO livers, respectively (Figure S3C). Thus, control of circadian gene expression by SIRT6 and SIRT1 appears to define unique subdomains of oscillating CCGs that are involved in distinct biological functions.

SIRT6 Interacts with CLOCK:BMAL1 and Controls Their Chromatin Recruitment

Because SIRT6 is reported to localize to actively transcribed genomic loci (Ram et al., 2011), we sought to decipher the molecular mechanism by which SIRT6 controls circadian transcription. Fractionated liver extracts that lack SIRT6 result in a drastic increase in BMAL1 association to chromatin, though the total amount of nucleoplasmic BMAL1 was unaltered (Figures 3A and S4). Also, *Bmal1* circadian expression is not altered in SIRT6 KO or SIRT1 KO, as compared to WT liver (Figure S3D).

Because BMAL1 association at chromatin is enhanced in the absence of SIRT6, we analyzed promoter-specific recruitment of the circadian machinery. Chromatin immunoprecipitation (ChIP) analysis was performed to understand whether recruitment of the circadian machinery was altered in the absence of SIRT6 or SIRT1, which would therefore contribute to altered CCG expression observed in our microarray analysis. Circadian BMAL1 recruitment to the *Rgs16* and *Mthfd1l* promoters is unaltered in the absence of SIRT1 (Figures 3B and 3C), despite the increased amplitude in gene expression in SIRT1 KO (Figure 2F). Schematic representation of the promoter, as well as selective recruitment of BMAL1 to different putative E boxes in the *Rgs16* and *Mthfd1l* promoters, is shown in Figure S5, illustrating that BMAL1 recruitment is virtually identical in WT and SIRT1 KO livers. In addition to *Rgs16* and *Mthfd1l*, BMAL1 recruitment is also unaltered at *Dbp* and *Per1* promoters in WT versus SIRT1 KO, despite the significant changes in circadian gene expression (Figure S6). In contrast, lack of SIRT6 results in a significant increase in circadian BMAL1 occupancy (ZT 4 and ZT 8) at the *Dbp* promoter (Figure 3D). A detailed schematic of the *Dbp* promoter illustrating select sites of circadian BMAL1 recruitment, as well as *Dbp* expression profile, is shown (Figure 3D). Also, an increase in

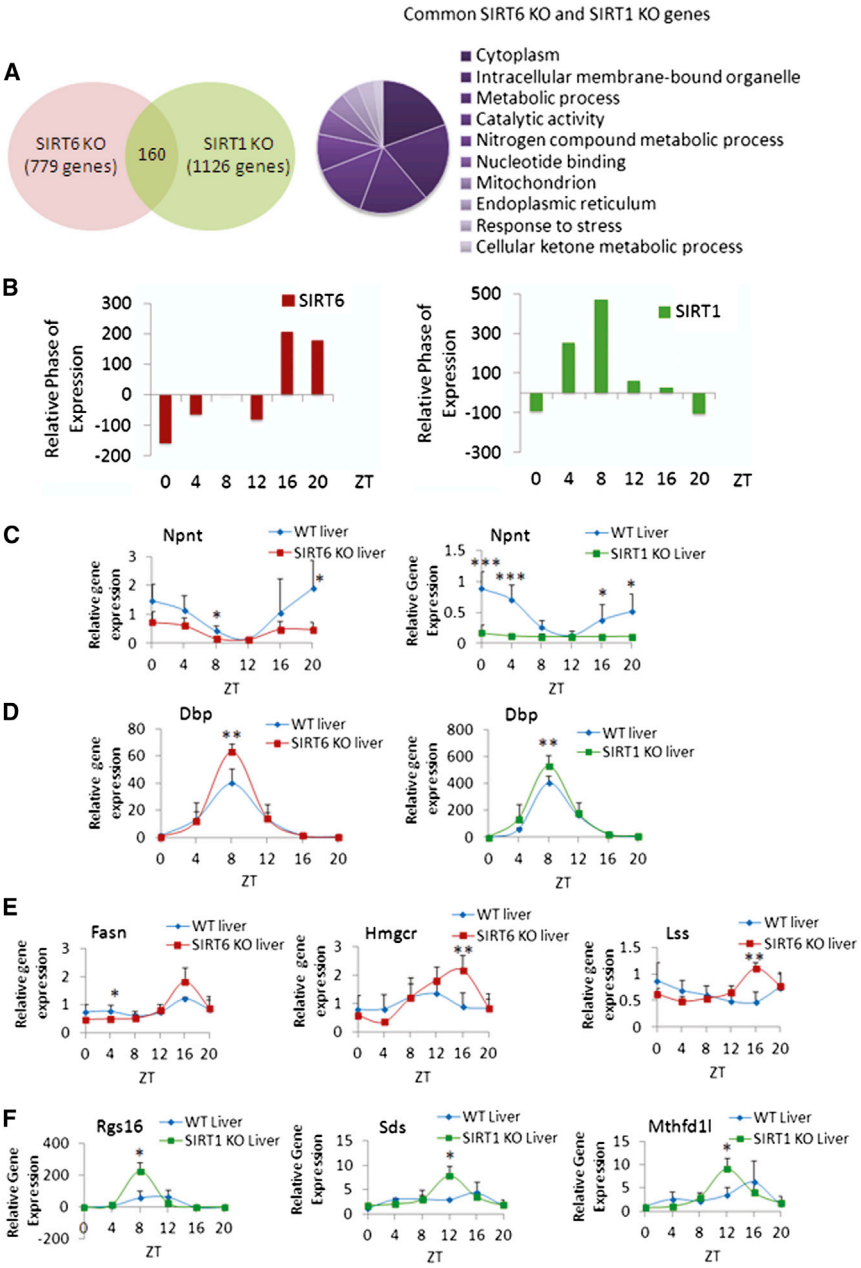

Figure 2. Comparison of SIRT6 and SIRT1-Dependent Circadian Gene Expression

(A) Venn diagram displays genes with common circadian expression profiles in SIRT6 KO and SIRT1 KO microarray data sets. Right panel illustrates GO terms enriched in the 160 common genes similarly regulated by SIRT6 and SIRT1. Top ten GO terms (molecular function, biological process, and cellular component) were selected based on a 0.01 p value cutoff using DAVID.

(B) Relative phase of expression of significant genes (p value < 0.01) from SIRT6 and SIRT1 microarray data. Phase of SIRT6 KO or SIRT1 KO genes at indicated ZTs is shown relative to WT.

(C) Gene expression profiles of *Npnt* in WT and SIRT6 KO or SIRT1 KO mouse liver based on quantitative real-time PCR analysis. Total RNA was extracted from three to five independent livers at indicated ZTs.

(D) Gene expression, based on real-time PCR, for *Dbp* in WT and SIRT6/SIRT1 disrupted livers.

(E) Expression profiles for *Fasn*, *Hmgcr*, and *Lss* genes with increased circadian amplitude exclusively in SIRT6 KO versus WT.

(F) Expression of genes oscillating more robustly only in SIRT1 KO livers versus WT, including *Rgs16*, *Sds*, and *Mthfd1l*. Gene expression was normalized relative to 18S rRNA expression. Error bars indicate SEM. Significance was calculated using Student's t test and *, **, and *** indicate p value cutoffs of 0.05, 0.01, and 0.001, respectively. Primer sequences used for gene expression analysis are in Table S2.

Ac-H3K9 across all time points is seen (Figure 3E). Additional data show altered BMAL1 recruitment to *Per1* and *Amd1* promoters in the absence of SIRT6 (Figure S7). To further address the effect of SIRT6, we used a *Dbp*-luciferase reporter and found that ectopic expression of SIRT6 results in dose-dependent dampening of CLOCK:BMAL1-driven transcription (Figure 3F), similar to results with SIRT1 (Bellet et al., 2013). Thus, differently from SIRT1, SIRT6 controls circadian function by operating directly at the transcription level by recruiting the clock machinery to chromatin.

Moreover, we sought to confirm that SIRT6 interacts with the circadian transcription complex. SIRT6 physically interacts with CLOCK and BMAL1, individually or together, as shown by coimmunoprecipitation (co-IP) (Figures 4A and 4B). Also, SIRT6 does not interact directly with SIRT1 by co-IP (Figure 4B). Furthermore, when CLOCK and BMAL1 are ectopically expressed with SIRT6 alone or in combination with both SIRT6 and SIRT1, the SIRT6 IP complex only interacts with CLOCK and BMAL1 and not SIRT1 (Figure 4C). Furthermore, by fractionating WT mouse liver, we reveal that subcellular localization of SIRT6 is predominantly in the nucleus and constitutively at chromatin at all ZTs, whereas SIRT1 is nuclear, but not chromatin bound (Figure 4D) (Mostoslavsky et al., 2006; Tennen et al., 2010). Likewise, co-IP experiments from chromatin fractions of HEK293 cells confirmed that SIRT1 does not reside at chromatin (Figure 4E). Also, the SIRT6-dependent interaction with CLOCK and BMAL1 is found at chromatin (Figure 4E). In addition, sequential co-IP experiments were performed to pull down the SIRT6- and SIRT1-dependent clock complexes from the same HEK293 cell lysates. Primary IP against Flag-SIRT1 revealed an interaction with CLOCK, and a secondary IP with HA-SIRT6 also revealed an interaction with CLOCK (Figure 4F), which is in keeping with evidence showing that these two sirtuins independently interact with the clock machinery. Lastly, SIRT1 has been shown to deacetylate BMAL1 at

lysine 537 (Hirayama et al., 2007; Nakahata et al., 2008). Whereas SIRT1 readily deacetylates BMAL1, SIRT6 is not able to do so (Figure 4G), highlighting different mechanisms of action of these two sirtuins that reside in partitioned subcellular clock complexes.

SIRT6 Controls SREBP-1-Dependent Circadian Transcription

Based on circadian gene expression profiles altered in SIRT6 KO liver, a number of genes were found to be SREBP targets such as *Fasn*, *Hmgcr*, and *Lss* (Figure 2D). MotifMap (Daily et al., 2011; Xie et al., 2009) was used to determine global transcription factor binding site enrichment in promoters with altered expression profiles when SIRT6 was disrupted. SREBP binding sites are highly enriched (137 sites) compared to serum response factor (SRF), peroxisome proliferator-activated receptor gamma (PPARγ), forkhead box (FOXO), or E26 transformation-specific (ETS) family motifs (Figure 5A). Next, genes whose expression is disrupted by loss of SIRT6 were compared to published ChIP-sequencing data (Seo et al., 2009, 2011) to determine the extent of SREBP-1 and SREBP-2 gene targets that overlap with SIRT6. In addition to the genes already mentioned, other SREBP targets appear disrupted in SIRT6 KO, including fatty acid elongase family members (*Elovl*), low-density lipoprotein receptor (*Ldlr*), and acetoacetyl-CoA synthetase (*Aacs*) genes (which are also represented in MotifMap SREBP hits). As a role for SIRT1 in SREBP signaling cannot be excluded, we compared SREBP-1 target genes (Seo et al., 2009) to SIRT6- and SIRT1-dependent gene targets (Table S1). Interestingly, overlapping genes between SIRT6/SREBP-1 targets were enriched in GO terms for fatty acid and lipid metabolism, whereas SIRT1/SREBP-1 overlapping targets were enriched in lipid and steroid metabolism (Figure 5A), suggesting a partition in biological function in SIRT1- or SIRT6-specific control of SREBP.

As there are no significant changes in SREBP-1c circadian transcript and protein levels in SIRT6 KO livers (Figure 5B), we carried out ChIP experiments. Strikingly, SREBP-1 circadian recruitment to the *Fasn* promoter, a known SREBP-responsive gene (Seo et al., 2009), is significantly increased in the absence of SIRT6, as compared to WT (Figure 5C). The increase is prominent at ZT 4, thereby preceding the peak of *Fasn* transcription at ZT 16, a scenario in keeping with accumulated evidence, especially in a circadian context (Koike et al., 2012; Rey et al., 2011). A schematic of the *Fasn* promoter illustrating selective SREBP-1 recruitment to the TSS versus negative control regions, as well as recruitment to the *Hmgcr* and *Lss* promoters, is shown (Figures 5C and S8). Also, an increase in Ac-H3K9 levels is present at the *Fasn* promoter across most ZTs (Figure 5C). Based on this evidence, it is expected that SREBP-1c contributes to *Fasn* circadian gene expression. To confirm this, we used livers from WT and SREBP-1c KO mice (Seo et al., 2009) at ZT 4 and ZT 16 and observed a significant dampening of *Fasn* circadian expression in SREBP-1c KO livers, whereas *Dbp* and *Rev-Erbα* circadian expression remains unaltered (Figure 5D). Thus, SIRT6 appears to define a class of genes whose amplitude in oscillation is directed by SREBP-1c. To functionally explore the effects of SIRT6 on SREBP-1c-mediated transcription, we used a luciferase reporter with either a full-length *Fasn* promoter (containing the previously described binding site of SREBP-1, referred to as Fas-Luc −1594/+65) (Bennett et al., 1995) or a mutant that disrupts SREBP-1 binding (Fas-Luc −65 MT) (Joseph et al., 2002). Coexpression with SREBP-1c showed robust *Fasn* promoter activation that is strongly repressed by increasing amounts of SIRT6 (Figure 5E). Importantly, the Fas-Luc −65 MT reporter is not sensitive to SIRT6-mediated repression. The effect is specific, as SIRT1 is not able to repress SREBP-1c-driven activation of *Fasn* (Figure 5E). Thus, SIRT6 is implicated in regulating proper SREBP-1c chromatin recruitment, resulting in circadian transcription of its target genes.

Sirtuin-Dependent Genomic Partitioning Results in Differential Circadian Metabolic Phenotypes

Metabolomics analysis was used to determine in an unbiased manner the physiological consequences of SIRT6 or SIRT1 disruption along the hepatic circadian cycle. Heat maps highlight oscillating metabolites (JTK_cycle < 0.05 p value cutoff) in WT livers that were disrupted in SIRT6 KO (left) and metabolites that oscillated more robustly in SIRT6 KO livers, as compared to WT (right) (Figure 6A). In total, 77 metabolites displayed a genotype-dependent effect in the SIRT6 metabolome, and 142 metabolites were dependent on circadian rhythmicity (Figure 6A). We also compared the metabolome profile obtained from the SIRT6 KO mice to livers from SIRT1 KO animals (Figure 6B). Heat maps illustrate the metabolomics data for SIRT1, with oscillating metabolites only in WT livers (left) and those found to oscillate robustly in SIRT1 KO (right). In the SIRT1 metabolome, 42 metabolites displayed a genotype effect, whereas 199 show a time-of-day-dependent effect. In total, 85 metabolites robustly oscillate exclusively in SIRT6 KO, and 57 metabolites display strong rhythmicity in SIRT1 KO livers.

Metabolites were grouped into biological functional categories (peptides, cofactors and vitamins, lipids, nucleotides, amino acids, and carbohydrates) to determine where significant changes occurred in the livers from SIRT6 KO and SIRT1 KO mice versus their WT littermates. The most robust change was seen in lipid-related metabolites in SIRT6 KO livers (Figure 6C). These lipids were heavily related to fatty acid metabolism, including circadian disruption of fatty acid synthesis (medium and long-chain fatty acids), storage, cellular membrane lipids, and signaling. Using SIRT6 microarray data, genes were run through DAVID to identify possible altered gene expression profiles that match in GO biological function with the metabolomics data set. A strong correlation in GO biological function was found (Figure 6D), comparing the high-throughput metabolome and transcriptome data when SIRT6 is disrupted (for detailed analysis consult CircadiOmics: http://circadiomics.igb.uci.edu [Patel et al., 2012]).

A group of lipids that displayed a strikingly enhanced circadian oscillation with a peak at ZT 16 was membrane lysolipids that are related to cellular synthesis or degradation. Also, genes encoding phospholipases related to lipid signaling displayed altered expression profiles with a paralleled change in eicosanoid metabolite rhythms in response to SIRT6 disruption, indicating that signaling/inflammatory events are SIRT6 regulated. As an example, genes of the phospholipase A2 family (*Pla2g2a* and *Pla2g12a*) gained circadian oscillation in the absence of SIRT6,

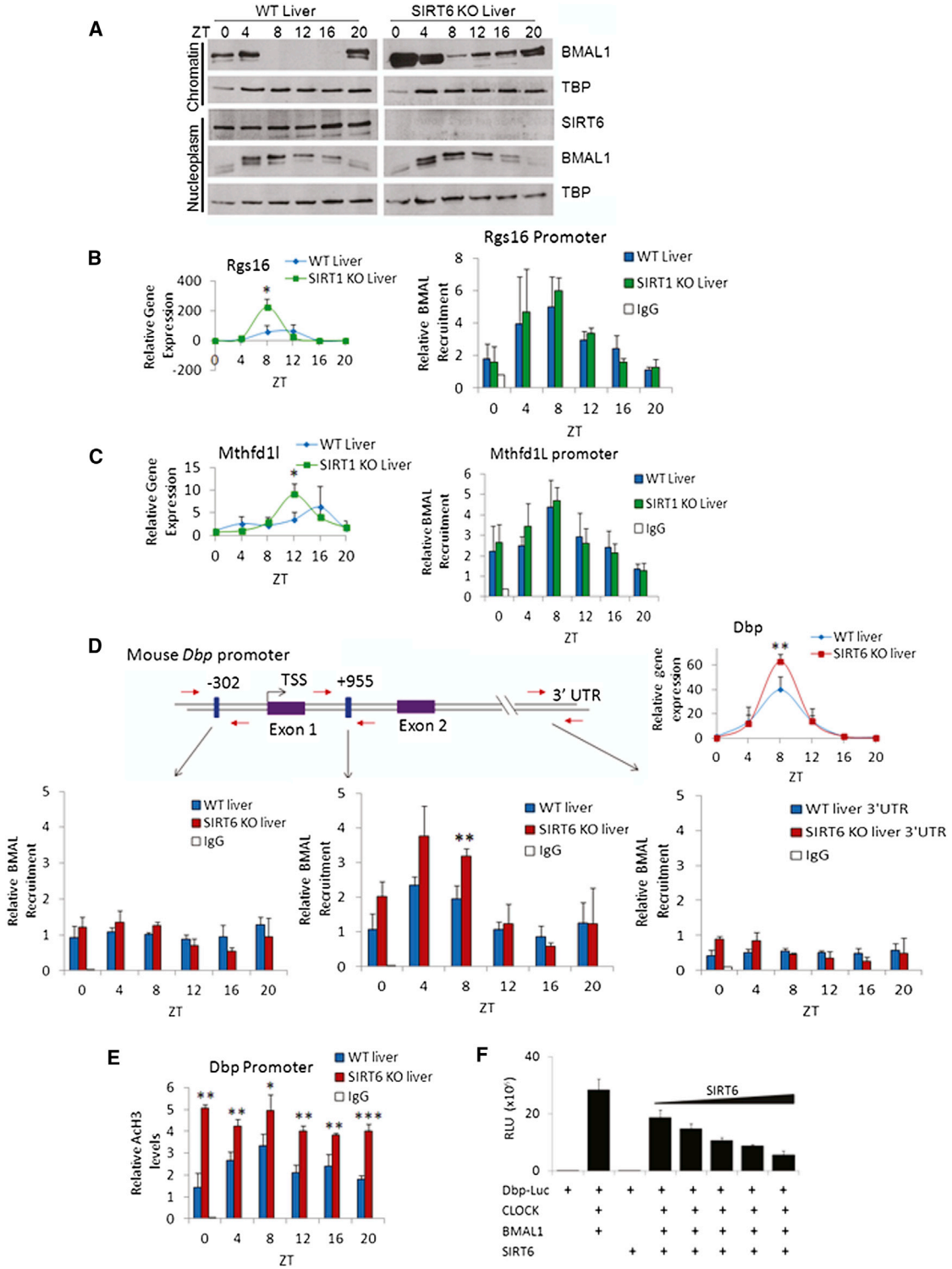

Figure 3. SIRT6 Regulates the Circadian Transcriptional Machinery

(A) Western analysis of fractionated liver (nucleoplasm and chromatin-enriched fractions) at indicated ZTs.

(B and C) ChIP analysis in WT and SIRT1 KO livers at indicated ZTs using n = 3 independent livers per genotype and time point. Left panels display gene expression profile, and right panels display BMAL1 recruitment to *Rgs16* and *Mthfd1l* gene promoters by ChIP, as compared to rabbit IgG negative control.

(legend continued on next page)

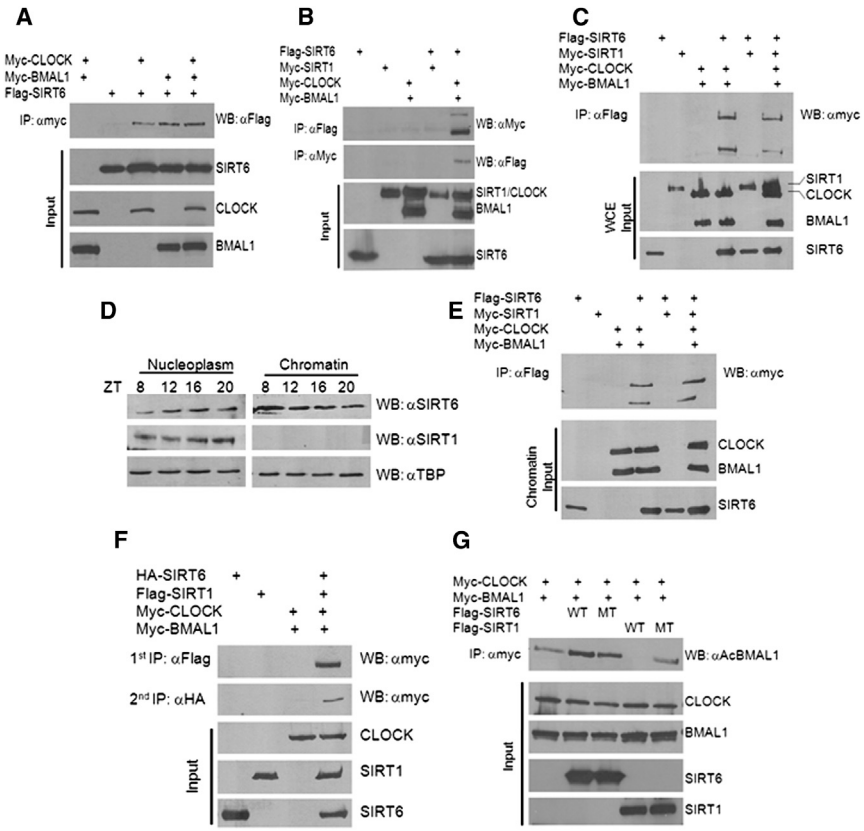

Figure 4. SIRT6, CLOCK, and BMAL1 Interact in an Exclusive Complex from SIRT1

(A and B) Co-IP experiments were performed in HEK293 cells by ectopically expressing myc-CLOCK, myc-BMAL1, flag-SIRT6, and myc-SIRT1. IP was performed with either anti-myc antibody or Flag-M2 agarose beads overnight, as indicated. Western was performed with anti-myc and anti-flag antibodies as indicated.

(C) myc-CLOCK and myc-BMAL1 were ectopically expressed in HEK293 cells with flag-SIRT6 alone or flag-SIRT6 + myc-SIRT1. Whole-cell extracts (WCEs) were used for Flag IP.

(D) WT liver was fractionated at the indicated ZTs, and nucleoplasmic and chromatin fractions were probed for endogenous SIRT6 and SIRT1 protein expression.

(E) myc-CLOCK and myc-BMAL1 were ectopically expressed in HEK293 cells with flag-SIRT6 alone or flag-SIRT6 + myc-SIRT1. Cells were fractionated and chromatin fraction was used for Flag IP.

(F) Sequential IPs were performed from HEK293 cells ectopically expressing HA-SIRT6, Flag-SIRT1, and myc-CLOCK. Primary IP was performed with Flag (SIRT1), and secondary IP from the same lysates was done with HA (SIRT6) to reveal myc-CLOCK interaction.

(G) BMAL1 acetylation assay was performed in HEK293 cells with ectopic expression of myc-CLOCK, myc-BMAL1, Flag-SIRT6, and Flag-SIRT1 (WT and catalytic mutant). IP was performed with anti-myc and Western with anti-Ac BMAL1 antibody.

which corresponded with circadian upregulation of downstream 15-HETE levels. In addition to *Fasn*, fatty acid elongases and fatty acid transporters were significantly altered in response to SIRT6 disruption. Both carnitine and acetylcarnitine, which are important for beta oxidation of fatty acids in the mitochondria, gain circadian oscillation and peak at ZT16 in the SIRT6 KO livers. Although synthesis and breakdown of fatty acid pathways are related to SIRT6, storage of fatty acids into triglycerides was also altered as evidenced by a gain in oscillation of *Agpat6* and glycerol-3-phosphate in the SIRT6 KO mice. These metabolite pathways parallel the altered SREBP transcriptional response and indicate that SIRT6 is required for proper circadian regulation of fatty acid synthesis, storage, breakdown, and signaling.

DISCUSSION

Circadian control of metabolism is thought to be critical for organismal homeostasis (Feng and Lazar, 2012; Sahar and Sassone-Corsi, 2012), and the identification of the molecular players implicated in this control is likely to reveal novel pharmacological strategies. Specifically, SIRT6 regulates hepatic circadian transcription consequently linked to downstream modulation of fatty acid metabolism (Figure 7). SIRT6 interacts with core clock proteins and controls circadian chromatin recruitment of BMAL1 to target promoters. Importantly, SIRT6 also controls SREBP-1 recruitment to target promoters, such as *Fasn*, and helps maintain proper cyclic transcription. In fact, circadian metabolomics analyses reveal that SIRT6 controls lipid metabolism, contributing to the regulation of pathways involved in fatty acid synthesis and beta oxidation, triglyceride storage, signaling, and cellular membrane lipids.

One conclusion of this study is that two sirtuins, SIRT6 and SIRT1, control distinct subdomains of the circadian genome through different mechanisms. SIRT6 has been reported to reside at transcriptionally active loci (Ram et al., 2011), and its chromatin association is dynamic in response to stimuli so as to activate specific biological classes of genes (Kawahara et al., 2011). It is tempting to speculate that SIRT6 operates

(D) BMAL1 ChIP analysis in WT and SIRT6 KO liver to the *Dbp* promoter and Intron 1. Schematic of the *Dbp* promoter: blue boxes illustrate locations of E boxes, and red arrows indicate locations of real-time PCR primers used for ChIP. Numbers shown above E boxes indicate locations relative to the TSS. *Dbp* expression is on the right. BMAL1 ChIP data illustrate recruitment to the *Dbp* promoter, Intron I, and 3′ UTR regions.

(E) AcH3 ChIP data at the *Dbp* Promoter in WT and SIRT6 KO livers at indicated ZTs.

(F) Luciferase assays were performed in JEG3 and HEK293 cells by ectopically expressing CLOCK, BMAL1, and SIRT6 with a *Dbp* luciferase reporter. 50–100 ng of CLOCK and BMAL1 expression plasmids were expressed with increasing amounts of SIRT6 (2–50 ng). Error bars indicate SEM. For real-time PCR and ChIP data, significance was calculated using Student's t test and *, **, and *** indicate p value cutoffs of 0.05, 0.01, and 0.001, respectively. Primer sequences used for gene expression and ChIP analysis are listed in Tables S2 and S3.

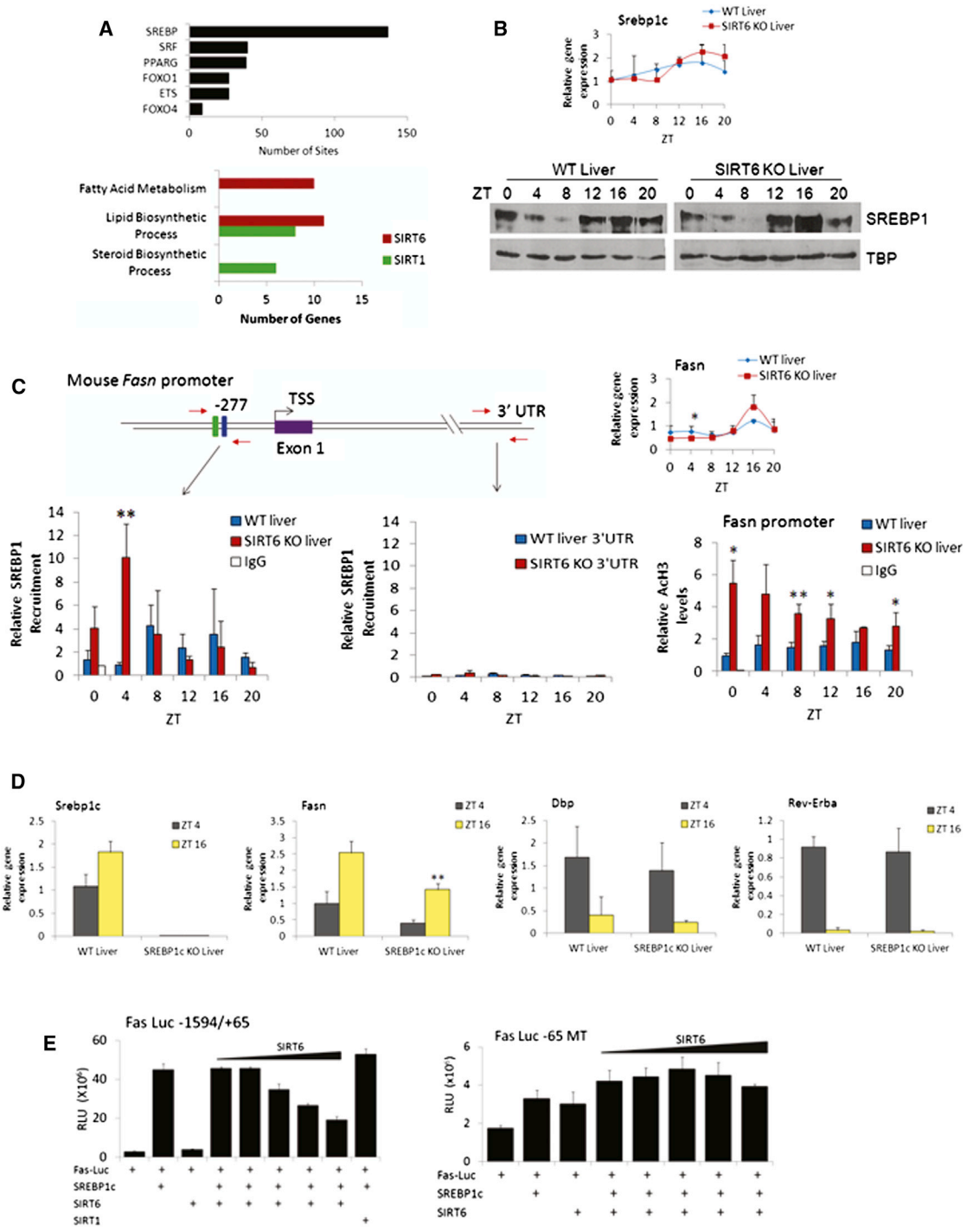

Figure 5. SIRT6 Modulates SREBP-Mediated Circadian Transcription

(A) MotifMap analysis of transcription factor binding sites enriched in gene promoters with altered expression when SIRT6 is disrupted (p value cutoff of 0.01 using JTK_cycle) (top). Search criteria were limited to 1 kb upstream of the TSS, with an FDR cutoff of 0.2 and a BBLS score of 0. Bottom displays overlapping SREBP1 target genes with SIRT6 and SIRT1-dependent genes. Genes are grouped in biological function by GO terms indicated.

(B) Gene expression as determined by real-time PCR and protein expression by western of Srebp-1c in WT and SIRT6 KO nuclear extracts.

(C) ChIP analysis on the *Fasn* promoter in WT and SIRT6 KO livers. Schematic of the *Fasn* promoter, with SRE-1 (green box) and E box (blue box) sites indicated. Right panel indicates *Fasn* gene expression, and bottom panel displays SREBP1 recruitment to the *Fasn* promoter and 3′ UTR by ChIP. AcH3 levels as determined by ChIP analysis at the *Fasn* promoter are shown.

(legend continued on next page)

as a transcriptional "marker," and given its HDAC function, it may have multiple roles in dictating the boundaries of transcription. As supporting evidence of this notion, we show that SIRT6 contributes to chromatin recruitment of both the circadian machinery, as well as SREBP-1. There is no evidence that SIRT1 functions in the same manner. Indeed, SIRT1 is not implicated in chromatin recruitment of the clock machinery (Figures 3, S5, and S6; Bellet et al., 2013). SIRT1 appears to modulate circadian transcription purely as a deacetylase by targeting both histone proteins and nonhistone proteins such as BMAL1 and PER2 (Asher et al., 2008; Nakahata et al., 2008). Intriguingly, free fatty acids (FFAs) are potent endogenous activators of SIRT6 HDAC activity, but not SIRT1 (Feldman et al., 2013). Thus, endogenous fatty acids could play a role in activating or sensitizing SIRT6, a notion that is particularly appealing, as our metabolomics data reveal that fatty acids peak in abundance at the beginning of the light phase (after feeding), which also coincides with peaks in BMAL1 and SREBP1 recruitment to chromatin (Figure 7). In keeping with this idea, the beginning of the light phase must therefore provide a permissive chromatin state, as recruitment of SIRT6-dependent transcription factors occurs primarily at ZT 4 and ZT 8 and in the case of SREBP-1 in advance of the peak in gene expression (Figures 3 and 5). Indeed, it has been proposed that an activated state of the circadian landscape exists between ZT 4 and ZT 12, when CLOCK:BMAL1 recruitment occurs and this active state is in advance of nascent transcription (Koike et al., 2012). In virtue of its tight chromatin association, SIRT6 could thereby operate by sensing changing cellular metabolite levels (NAD^+ or fatty acids) and translate this information to control circadian transcription. In this respect, SIRT6 would be unique among sirtuins because SIRT1 (Asher et al., 2008; Chang and Guarente, 2013; Nakahata et al., 2008) and SIRT3 (Peek et al., 2013) appear to be implicated in circadian regulation uniquely through their enzymatic function.

Aside from transcriptional/translational regulation of the clock, enzymatic activity of a number of factors influences circadian rhythms and could also contribute to SIRT6 function. SIRT6 was recently reported to directly regulate SREBP cleavage to its mature protein form as a result of SIRT6 localization to the promoters of genes such as SREBP cleavage-activating protein (SCAP) and site-1/2 proteases (S1P and S2P), which are involved in SREBP proteolytic cleavage and transport from the endoplasmic reticulum (ER)/Golgi apparatus (Elhanati et al., 2013). In addition to the circadian regulation of the SREBP lipogenic transcriptional program (Le Martelot et al., 2009), enzymatic regulation at the ER has been described whereby a secondary 12 hr rhythm in the unfolded protein response (UPR) pathway activates SREBP signaling and deregulates lipid metabolism (Cretenet et al., 2010). Though we are looking at 24 hr rhythms, these results highlight a possible connection that could further link SIRT6, SREBP, and ER-dependent enzymatic pathways that, in time, may contribute to the transcriptional role of SIRT6 and the clock described here.

Various mouse models have delineated the role of SREBP transcription factors in the lipogenic program (Horton et al., 2003; Seo et al., 2009, 2011). SREBP-1a and SREBP-1c (the form dominantly expressed in liver) activate both genes involved in fatty acid synthesis and the subsequent incorporation into triglycerides for storage and inclusion into cellular membranes. SREBP-2 is primarily implicated in cholesterol biosynthesis. Based on the results obtained by metabolomics analysis, our data indicate a disruption in fatty acid synthesis, breakdown, incorporation into membrane lipids, and storage with little disruption in cholesterol related pathways. Although we do not exclude the role of other factors such as hepatocyte nuclear factor 4 (HNF-4), liver X receptor (LXR), and peroxisome proliferator-activated receptors (PPARs), our results (Figures 5 and 6) point to SREBP-1c as a dominant player implicated in SIRT6 circadian regulation of fatty acid metabolism. Intriguingly, Kanfi et al. (2010) reported that, when transgenic mice overexpressing SIRT6 were challenged with a high-fat diet (HFD), these mice were protected from diet-induced obesity due to SIRT6 repression of PPARγ-target genes. In this respect, recent results from our laboratory have shown that HFD regimen in mice reprograms the hepatic circadian transcriptome by inducing de novo oscillations of PPARγ-dependent genes (Eckel-Mahan et al., 2013). Given the seemingly ubiquitous localization of SIRT6 at transcriptionally active genomic loci (Kawahara et al., 2011; Ram et al., 2011) and its role as a regulator of circadian transcription and SREBP signaling, SIRT6 could also be implicated in diet-induced metabolic regulation of SREBP, PPARs, or other factors. The remarkable role of SIRT6 in regulating the circadian transcriptome and defining a landscape for biologically relevant genomic loci places this epigenetic regulator in a central position to control the extensive circadian lipid metabolic program in the liver.

EXPERIMENTAL PROCEDURES

Animal Housing and Experimental Design

Liver-specific SIRT6 KO mice (Kim et al., 2010) and liver-specific SIRT1 KO mice (Nakahata et al., 2008) were previously described. All experiments were performed in accordance to the Institutional Animal Care and Use Committee (IACUC) guidelines at UCI. Animals were housed in a 12 hr light/dark paradigm and fed ad libitum.

DNA Microarray Analysis

Microarray analysis was performed at the UCI Genomics High-Throughput Facility. For detailed methodology, refer to the Extended Experimental Procedures.

(D) Gene expression as determined by real-time PCR of *Srebp-1c*, *Fasn*, *Dbp*, and *Rev-Erb*α at ZT4 and ZT16 in WT and SREBP-1c KO livers. Gene expression was normalized relative to 18S rRNA expression.

(E) Luciferase assays in JEG3 and HEK293 cells using two different *Fasn* luciferase reporters ectopically expressed with SREBP-1c (50 ng), SIRT6 (2–50 ng) or SIRT1 (50 ng). Left panel displays data using the *Fasn-Luc* −1594/+65 reporter, which contains the SRE binding site for SREBP1c-mediated transcription. Right panel shows luciferase activity using the *Fas-Luc* −65 MT reporter. Error bars indicate SEM. For real-time PCR and ChIP data, significance was calculated using Student's t test, and *, **, and *** indicate p value cutoffs of 0.05, 0.01, and 0.001, respectively. Primer sequences used for gene expression and ChIP analysis are listed in Tables S2 and S3.

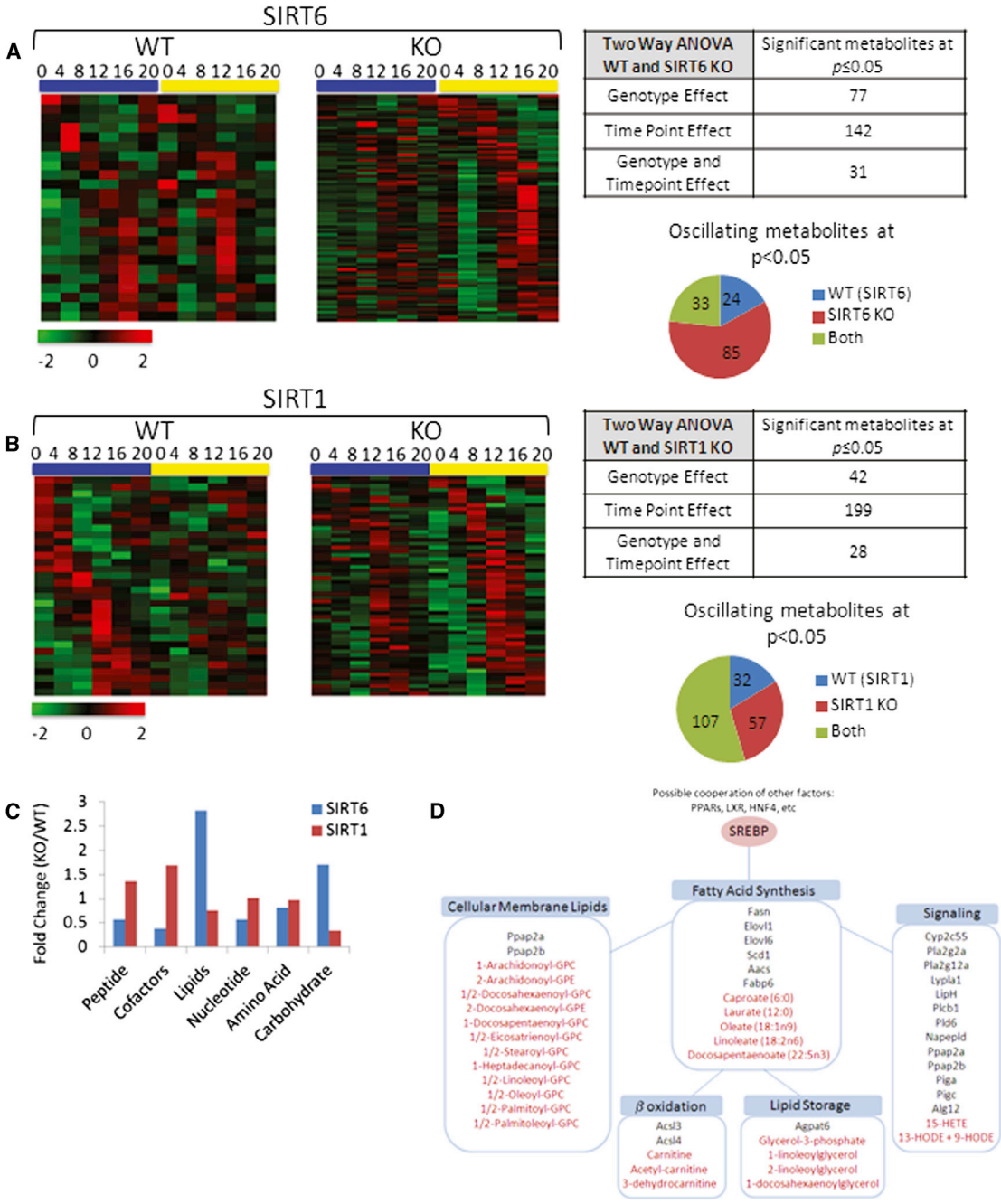

Figure 6. The SIRT6 and SIRT1 Circadian Metabolomes

(A and B) Heat maps displaying oscillating metabolites as determined by JTK_cycle (p value < 0.05) for SIRT6 (A) and SIRT1 (B) metabolomes. Left panels display circadian metabolites exclusively in WT liver, and right panels show metabolites with more robust oscillation when the sirtuin is disrupted. Tables and pie charts indicate number of significant metabolites using ANOVA and JTK_cycle at p value < 0.05 for time point and genotype.

(C) Biological classification of significant circadian metabolites for SIRT6 and SIRT1. Metabolites were grouped into six biological classifications indicated, and total numbers of significant metabolites in SIRT KOs were normalized to WT livers.

(D) Fatty acid metabolic pathways are outlined, and significantly disrupted genes or metabolites for SIRT6 are shown. Genes are indicated in black, and metabolites are indicated in red font.

Biological Pathway Analysis

The Database for Annotation, Visualization, and Integrated Discovery (DAVID) (Huang da et al., 2009a, 2009b) was used to identify GO terms related to biological process and molecular function related to our gene lists of interest.

Gene Expression Analysis

Equal amounts of total RNA were reverse transcribed to cDNA using iScript cDNA synthesis kit (Bio-Rad Laboratories, Hercules), according to manufacturer's protocol. cDNA was used for quantitative real-time PCR using iQ

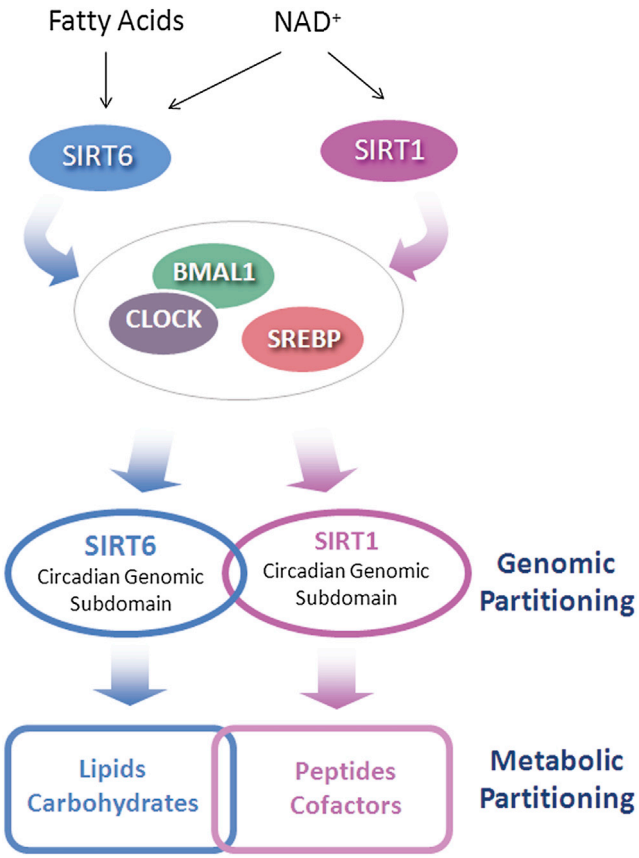

Figure 7. SIRT6 versus SIRT1-Dependent Circadian Functions
Scheme representing diverging functions of SIRT6 and SIRT1 in controlling circadian gene expression and metabolism. Different control mechanisms result in a SIRT6- and SIRT1-specific partitioning of the circadian genome that is paralleled by differential metabolic phenotypes.

SYBR green supermix (Bio-Rad Laboratories). Gene expression was normalized to 18S ribosomal RNA. Primers sequences used for gene expression analysis were designed with Primer3 software (Rozen and Skaletsky, 2000) and are listed in Table S2.

Chromatin Immunoprecipitation

Liver samples were quickly minced in PBS containing 1 mM $MgCl_2$ and protease inhibitor cocktail (Roche Applied Science, Indianapolis). Livers were homogenized and crosslinked with 2 mM disuccinimidyl glutarate (DSG) for 30 min at room temperature followed by a secondary crosslink step using 1% formaldehyde for 15 min. Crosslinking was quenched with 0.125 M glycine. For detailed methodology, refer to the Extended Experimental Procedures.

Western Blot Analysis

Livers were homogenized in RIPA lysis buffer containing protease inhibitor cocktail, NaF, and PMSF, sonicated briefly, and rocked to lyse cells at 4°C. Transfected cells were harvested in RIPA and similarly rocked to lyse cells. 35–50 μg of protein lysate was resolved on 10% SDS-PAGE. Antibodies used for western blots or IP include: SIRT6 and TBP (Abcam), AcBMAL1, SIRT1, and Myc (Millipore), Flag (Sigma-Aldrich), and SREBP-1 (Santa Cruz and kind gift from Dr. Timothy Osborne).

Plasmids and Luciferase Reporter Assays

JEG3 cells were transfected with 50–100 ng myc-BMAL1, myc-CLOCK (plasmids previously described [Katada and Sassone-Corsi, 2010]), Flag-SREBP1c (generous gift from Dr. Timothy Osborne), or Flag-SIRT6 (kind gift from Dr. Katrin Chua) in 24-well plate format. LacZ was also ectopically expressed with either Dbp-Luc (Kiyohara et al., 2008), Fasn-Luc −1594/+65, or Fasn-Luc −65 MT (Bennett et al., 1995; Joseph et al., 2002). For detailed methodology, refer to the Extended Experimental Procedures.

Mass Spectrometry for Metabolomics Analysis

Metabolomics analysis was carried out by Metabolon (Durham) using published methodology (Evans et al., 2009). For detailed methodology, refer to the Extended Experimental Procedures.

Statistical Analysis and MotifMap

For analysis of rhythmic genes and metabolites, the nonparametric test JTK_CYCLE was used incorporating a window of 20–28 hr for the determination of circadian periodicity (Hughes et al., 2010), including amplitude and phase analysis. A gene was considered circadian if at least one of its transcripts passed a p value cutoff of 0.01, whereas metabolites were considered circadian at a p value cutoff of 0.05. MotifMap (Daily et al., 2011; Xie et al., 2009) was used to determine enriched transcription factor binding sites in the microarray data sets using a false discovery rate (FDR) of 0.1 and a BBLS cutoff of 0.25 and searching within 1 kb of the TSS.

ACCESSION NUMBERS

The GEO accession number for the microarray data set is GSE57830.

SUPPLEMENTAL INFORMATION

Supplemental Information includes Extended Experimental Procedures, eight figures, and three tables and can be found with this article online at http://dx.doi.org/10.1016/j.cell.2014.06.050.

ACKNOWLEDGMENTS

We thank Katrin Chua for reagents and helpful discussions. We thank all members of the Sassone-Corsi lab and Melanie Oakes, Seung-Ah Chung, Valentina Ciobanu, Yuzo Kanomata, and Andrea Eckhart for helpful discussion and technical assistance. Funding for S.M. was provided by NIH postdoctoral fellowship GM097899. Funding for P.B. was provided by NSF (IIS-1321053) and NIH (LM010235 and LM07443). Financial support for P.S.-C. was provided by NIH (AG043745), Merieux Research Grant (53923), and Sirtris Pharmaceuticals (SP-48984).

Received: February 13, 2014
Revised: April 29, 2014
Accepted: June 20, 2014
Published: July 31, 2014

REFERENCES

Asher, G., Gatfield, D., Stratmann, M., Reinke, H., Dibner, C., Kreppel, F., Mostoslavsky, R., Alt, F.W., and Schibler, U. (2008). SIRT1 regulates circadian clock gene expression through PER2 deacetylation. Cell *134*, 317–328.

Belden, W.J., Lewis, Z.A., Selker, E.U., Loros, J.J., and Dunlap, J.C. (2011). CHD1 remodels chromatin and influences transient DNA methylation at the clock gene frequency. PLoS Genet. *7*, e1002166.

Bellet, M.M., Nakahata, Y., Boudjelal, M., Watts, E., Mossakowska, D.E., Edwards, K.A., Cervantes, M., Astarita, G., Loh, C., Ellis, J.L., et al. (2013). Pharmacological modulation of circadian rhythms by synthetic activators of the deacetylase SIRT1. Proc. Natl. Acad. Sci. USA *110*, 3333–3338.

Bennett, M.K., Lopez, J.M., Sanchez, H.B., and Osborne, T.F. (1995). Sterol regulation of fatty acid synthase promoter. Coordinate feedback regulation of two major lipid pathways. J. Biol. Chem. *270*, 25578–25583.

Chang, H.C., and Guarente, L. (2013). SIRT1 mediates central circadian control in the SCN by a mechanism that decays with aging. Cell *153*, 1448–1460.

Chang, H.C., and Guarente, L. (2014). SIRT1 and other sirtuins in metabolism. Trends Endocrinol. Metab. *25*, 138–145.

Cretenet, G., Le Clech, M., and Gachon, F. (2010). Circadian clock-coordinated 12 Hr period rhythmic activation of the IRE1alpha pathway controls lipid metabolism in mouse liver. Cell Metab. *11*, 47–57.

Daily, K., Patel, V.R., Rigor, P., Xie, X., and Baldi, P. (2011). MotifMap: integrative genome-wide maps of regulatory motif sites for model species. BMC Bioinformatics *12*, 495.

DiTacchio, L., Le, H.D., Vollmers, C., Hatori, M., Witcher, M., Secombe, J., and Panda, S. (2011). Histone lysine demethylase JARID1a activates CLOCK-BMAL1 and influences the circadian clock. Science *333*, 1881–1885.

Doi, M., Hirayama, J., and Sassone-Corsi, P. (2006). Circadian regulator CLOCK is a histone acetyltransferase. Cell *125*, 497–508.

Dominy, J.E., Jr., Lee, Y., Jedrychowski, M.P., Chim, H., Jurczak, M.J., Camporez, J.P., Ruan, H.B., Feldman, J., Pierce, K., Mostoslavsky, R., et al. (2012). The deacetylase Sirt6 activates the acetyltransferase GCN5 and suppresses hepatic gluconeogenesis. Mol. Cell *48*, 900–913.

Duong, H.A., Robles, M.S., Knutti, D., and Weitz, C.J. (2011). A molecular mechanism for circadian clock negative feedback. Science *332*, 1436–1439.

Eckel-Mahan, K.L., Patel, V.R., de Mateo, S., Orozco-Solis, R., Ceglia, N.J., Sahar, S., Dilag-Penilla, S.A., Dyar, K.A., Baldi, P., and Sassone-Corsi, P. (2013). Reprogramming of the circadian clock by nutritional challenge. Cell *155*, 1464–1478.

Elhanati, S., Kanfi, Y., Varvak, A., Roichman, A., Carmel-Gross, I., Barth, S., Gibor, G., and Cohen, H.Y. (2013). Multiple regulatory layers of SREBP1/2 by SIRT6. Cell Rep. *4*, 905–912.

Etchegaray, J.P., Lee, C., Wade, P.A., and Reppert, S.M. (2003). Rhythmic histone acetylation underlies transcription in the mammalian circadian clock. Nature *421*, 177–182.

Evans, A.M., DeHaven, C.D., Barrett, T., Mitchell, M., and Milgram, E. (2009). Integrated, nontargeted ultrahigh performance liquid chromatography/electrospray ionization tandem mass spectrometry platform for the identification and relative quantification of the small-molecule complement of biological systems. Anal. Chem. *81*, 6656–6667.

Feldman, J.L., Baeza, J., and Denu, J.M. (2013). Activation of the protein deacetylase SIRT6 by long-chain fatty acids and widespread deacylation by mammalian sirtuins. J. Biol. Chem. *288*, 31350–31356.

Feng, D., and Lazar, M.A. (2012). Clocks, metabolism, and the epigenome. Mol. Cell *47*, 158–167.

Finkel, T., Deng, C.X., and Mostoslavsky, R. (2009). Recent progress in the biology and physiology of sirtuins. Nature *460*, 587–591.

Gil, R., Barth, S., Kanfi, Y., and Cohen, H.Y. (2013). SIRT6 exhibits nucleosome-dependent deacetylase activity. Nucleic Acids Res. *41*, 8537–8545.

Gut, P., and Verdin, E. (2013). The nexus of chromatin regulation and intermediary metabolism. Nature *502*, 489–498.

Hall, J.A., Dominy, J.E., Lee, Y., and Puigserver, P. (2013). The sirtuin family's role in aging and age-associated pathologies. J. Clin. Invest. *123*, 973–979.

Hirayama, J., Sahar, S., Grimaldi, B., Tamaru, T., Takamatsu, K., Nakahata, Y., and Sassone-Corsi, P. (2007). CLOCK-mediated acetylation of BMAL1 controls circadian function. Nature *450*, 1086–1090.

Horton, J.D., Shah, N.A., Warrington, J.A., Anderson, N.N., Park, S.W., Brown, M.S., and Goldstein, J.L. (2003). Combined analysis of oligonucleotide microarray data from transgenic and knockout mice identifies direct SREBP target genes. Proc. Natl. Acad. Sci. USA *100*, 12027–12032.

Houtkooper, R.H., Pirinen, E., and Auwerx, J. (2012). Sirtuins as regulators of metabolism and healthspan. Nat. Rev. Mol. Cell Biol. *13*, 225–238.

Huang da, W., Sherman, B.T., and Lempicki, R.A. (2009a). Bioinformatics enrichment tools: paths toward the comprehensive functional analysis of large gene lists. Nucleic Acids Res. *37*, 1–13.

Huang da, W., Sherman, B.T., and Lempicki, R.A. (2009b). Systematic and integrative analysis of large gene lists using DAVID bioinformatics resources. Nat. Protoc. *4*, 44–57.

Hughes, M.E., Hogenesch, J.B., and Kornacker, K. (2010). JTK_CYCLE: an efficient nonparametric algorithm for detecting rhythmic components in genome-scale data sets. J. Biol. Rhythms *25*, 372–380.

Joseph, S.B., Laffitte, B.A., Patel, P.H., Watson, M.A., Matsukuma, K.E., Walczak, R., Collins, J.L., Osborne, T.F., and Tontonoz, P. (2002). Direct and indirect mechanisms for regulation of fatty acid synthase gene expression by liver X receptors. J. Biol. Chem. *277*, 11019–11025.

Kanfi, Y., Peshti, V., Gil, R., Naiman, S., Nahum, L., Levin, E., Kronfeld-Schor, N., and Cohen, H.Y. (2010). SIRT6 protects against pathological damage caused by diet-induced obesity. Aging Cell *9*, 162–173.

Katada, S., and Sassone-Corsi, P. (2010). The histone methyltransferase MLL1 permits the oscillation of circadian gene expression. Nat. Struct. Mol. Biol. *17*, 1414–1421.

Katada, S., Imhof, A., and Sassone-Corsi, P. (2012). Connecting threads: epigenetics and metabolism. Cell *148*, 24–28.

Kawahara, T.L., Michishita, E., Adler, A.S., Damian, M., Berber, E., Lin, M., McCord, R.A., Ongaigui, K.C., Boxer, L.D., Chang, H.Y., and Chua, K.F. (2009). SIRT6 links histone H3 lysine 9 deacetylation to NF-kappaB-dependent gene expression and organismal life span. Cell *136*, 62–74.

Kawahara, T.L., Rapicavoli, N.A., Wu, A.R., Qu, K., Quake, S.R., and Chang, H.Y. (2011). Dynamic chromatin localization of Sirt6 shapes stress- and aging-related transcriptional networks. PLoS Genet. *7*, e1002153.

Kim, H.S., Xiao, C., Wang, R.H., Lahusen, T., Xu, X., Vassilopoulos, A., Vazquez-Ortiz, G., Jeong, W.I., Park, O., Ki, S.H., et al. (2010). Hepatic-specific disruption of SIRT6 in mice results in fatty liver formation due to enhanced glycolysis and triglyceride synthesis. Cell Metab. *12*, 224–236.

Kiyohara, Y.B., Nishii, K., Ukai-Tadenuma, M., Ueda, H.R., Uchiyama, Y., and Yagita, K. (2008). Detection of a circadian enhancer in the mDbp promoter using prokaryotic transposon vector-based strategy. Nucleic Acids Res. *36*, e23.

Koike, N., Yoo, S.H., Huang, H.C., Kumar, V., Lee, C., Kim, T.K., and Takahashi, J.S. (2012). Transcriptional architecture and chromatin landscape of the core circadian clock in mammals. Science *338*, 349–354.

Le Martelot, G., Claudel, T., Gatfield, D., Schaad, O., Kornmann, B., Lo Sasso, G., Moschetta, A., and Schibler, U. (2009). REV-ERBalpha participates in circadian SREBP signaling and bile acid homeostasis. PLoS Biol. *7*, e1000181.

Masri, S., and Sassone-Corsi, P. (2010). Plasticity and specificity of the circadian epigenome. Nat. Neurosci. *13*, 1324–1329.

Michishita, E., McCord, R.A., Berber, E., Kioi, M., Padilla-Nash, H., Damian, M., Cheung, P., Kusumoto, R., Kawahara, T.L., Barrett, J.C., et al. (2008). SIRT6 is a histone H3 lysine 9 deacetylase that modulates telomeric chromatin. Nature *452*, 492–496.

Michishita, E., McCord, R.A., Boxer, L.D., Barber, M.F., Hong, T., Gozani, O., and Chua, K.F. (2009). Cell cycle-dependent deacetylation of telomeric histone H3 lysine K56 by human SIRT6. Cell Cycle *8*, 2664–2666.

Mostoslavsky, R., Chua, K.F., Lombard, D.B., Pang, W.W., Fischer, M.R., Gellon, L., Liu, P., Mostoslavsky, G., Franco, S., Murphy, M.M., et al. (2006). Genomic instability and aging-like phenotype in the absence of mammalian SIRT6. Cell *124*, 315–329.

Nakahata, Y., Kaluzova, M., Grimaldi, B., Sahar, S., Hirayama, J., Chen, D., Guarente, L.P., and Sassone-Corsi, P. (2008). The NAD+-dependent deacetylase SIRT1 modulates CLOCK-mediated chromatin remodeling and circadian control. Cell *134*, 329–340.

Patel, V.R., Eckel-Mahan, K., Sassone-Corsi, P., and Baldi, P. (2012). CircadiOmics: integrating circadian genomics, transcriptomics, proteomics and metabolomics. Nat. Methods *9*, 772–773.

Peek, C.B., Affinati, A.H., Ramsey, K.M., Kuo, H.Y., Yu, W., Sena, L.A., Ilkayeva, O., Marcheva, B., Kobayashi, Y., Omura, C., et al. (2013). Circadian clock NAD+ cycle drives mitochondrial oxidative metabolism in mice. Science *342*, 1243417.

Ram, O., Goren, A., Amit, I., Shoresh, N., Yosef, N., Ernst, J., Kellis, M., Gymrek, M., Issner, R., Coyne, M., et al. (2011). Combinatorial patterning of chromatin regulators uncovered by genome-wide location analysis in human cells. Cell *147*, 1628–1639.

Rey, G., Cesbron, F., Rougemont, J., Reinke, H., Brunner, M., and Naef, F. (2011). Genome-wide and phase-specific DNA-binding rhythms of BMAL1 control circadian output functions in mouse liver. PLoS Biol. *9*, e1000595.

Ripperger, J.A., and Schibler, U. (2006). Rhythmic CLOCK-BMAL1 binding to multiple E-box motifs drives circadian Dbp transcription and chromatin transitions. Nat. Genet. *38*, 369–374.

Rozen, S., and Skaletsky, H. (2000). Primer3 on the WWW for general users and for biologist programmers. Methods Mol. Biol. *132*, 365–386.

Sahar, S., and Sassone-Corsi, P. (2012). Regulation of metabolism: the circadian clock dictates the time. Trends Endocrinol. Metab. *23*, 1–8.

Seo, Y.K., Chong, H.K., Infante, A.M., Im, S.S., Xie, X., and Osborne, T.F. (2009). Genome-wide analysis of SREBP-1 binding in mouse liver chromatin reveals a preference for promoter proximal binding to a new motif. Proc. Natl. Acad. Sci. USA *106*, 13765–13769.

Seo, Y.K., Jeon, T.I., Chong, H.K., Biesinger, J., Xie, X., and Osborne, T.F. (2011). Genome-wide localization of SREBP-2 in hepatic chromatin predicts a role in autophagy. Cell Metab. *13*, 367–375.

Tennen, R.I., and Chua, K.F. (2011). Chromatin regulation and genome maintenance by mammalian SIRT6. Trends Biochem. Sci. *36*, 39–46.

Tennen, R.I., Berber, E., and Chua, K.F. (2010). Functional dissection of SIRT6: identification of domains that regulate histone deacetylase activity and chromatin localization. Mech. Ageing Dev. *131*, 185–192.

Toiber, D., Erdel, F., Bouazoune, K., Silberman, D.M., Zhong, L., Mulligan, P., Sebastian, C., Cosentino, C., Martinez-Pastor, B., Giacosa, S., et al. (2013). SIRT6 recruits SNF2H to DNA break sites, preventing genomic instability through chromatin remodeling. Mol. Cell *51*, 454–468.

Wijnen, H., and Young, M.W. (2006). Interplay of circadian clocks and metabolic rhythms. Annu. Rev. Genet. *40*, 409–448.

Xiao, C., Kim, H.S., Lahusen, T., Wang, R.H., Xu, X., Gavrilova, O., Jou, W., Gius, D., and Deng, C.X. (2010). SIRT6 deficiency results in severe hypoglycemia by enhancing both basal and insulin-stimulated glucose uptake in mice. J. Biol. Chem. *285*, 36776–36784.

Xie, X., Rigor, P., and Baldi, P. (2009). MotifMap: a human genome-wide map of candidate regulatory motif sites. Bioinformatics *25*, 167–174.

Yang, B., Zwaans, B.M., Eckersdorff, M., and Lombard, D.B. (2009). The sirtuin SIRT6 deacetylates H3 K56Ac in vivo to promote genomic stability. Cell Cycle *8*, 2662–2663.

Zhong, L., D'Urso, A., Toiber, D., Sebastian, C., Henry, R.E., Vadysirisack, D.D., Guimaraes, A., Marinelli, B., Wikstrom, J.D., Nir, T., et al. (2010). The histone deacetylase Sirt6 regulates glucose homeostasis via Hif1alpha. Cell *140*, 280–293.

Cell

EXTENDED EXPERIMENTAL PROCEDURES

DNA Microarray Analysis

Microarray analysis was performed at the UCI Genomics High throughput Facility. Total RNA was extracted from 3 independent livers of age matched male mice (per genotype and ZT) using Trizol reagent (GIBCO BRL Life Technologies, Rockville, MD) and RNA was cleaned with QIAGEN RNeasy kit (QIAGEN, Chatsworth, CA). The Ambion WT expression kit (Life Technologies, Carlsbad, CA) was used to prepare cDNA which was hybridized to Affymetrix GeneChip 2.0ST arrays (Affymetrix, Santa Clara, CA). The GeneChip arrays were washed and then stained with streptavidin-phycoerythrin on an Affymetrix Fluidics Station 450 and arrays were scanned using GeneChip Scanner 3000 7G and Command Console Software v. 3.2.3 to produce .CEL intensity files. The probe cell intensity files (.CEL) were analyzed in Affymetrix Expression Console software v1.1.1 using the PLIER algorithm to generate probe level summarization files (.CHP).

Chromatin Immunoprecipitation

Liver nuclei were isolated first by washing cells, incubating in cell lysis buffer (5 mM HEPES, pH8, 85 mM KCl and 0.5% NP-40) and then in RIPA on ice. Nuclei were sonicated to fragment DNA for 10-15 cycles, amplitude of 30 on a Misonix ultrasonic liquid processor (Misonix Inc., Farmingdale, NY). Fragmented DNA was pre-cleared for 2 hr with protein G sepharose beads (Sigma-Aldrich, St. Louis, MO) and IP with antibody was setup overnight. Next day protein G beads were added for 3 hr and beads were subsequently washed with low salt, high salt, LiCl, and TE wash buffers (buffers recipes from EMD Millipore). Samples were reverse crosslinked in elution buffer (10 mM Tris-HCl, pH 8, 300 mM NaCl, 5 mM EDTA pH 8, and 0.5% SDS) overnight at 65°C. DNA was purified by phenol/chloroform and eluted in water for quantitative real-time PCR. Antibodies used were: BMAL1 (Abcam), SREBP-1 (Santa Cruz and gift from Dr. Timothy Osborne) and Histone H3K9ac (Active Motif). Primers for ChIP are listed in Table S3.

Luciferase Reporter Assays

Post-transfection of HEK293 cells with luciferase reporters and expression plasmids for CLOCK, BMAL1, SIRT6, SIRT1 and SREBP-1c, cells were lysed with luciferase lysis buffer (25 mM Tris-Phosphate pH 7.8, 2 mM EDTA, 1 mM DTT, 10% glycerol and 1% Triton X-100). Equal amounts of cell lysate and luciferase reaction buffer (20 mM Tris-phosphate pH 7.8, 1 mM $MgCl_2$, 2.5 mM $MgSO_4$, 0.1 mM EDTA, 33.3 mM DTT, 10 mM luciferin, 100 mM ATP and 10 mM coenzyme A) were mixed and assays were read on a Veritas microplate luminometer (Promega, Madison, WI). Beta-galactosidase assays were used to normalize luciferase light units.

Mass Spectrometry for Metabolomics Analysis

Metabolomics analysis was carried out by Metabolon, Inc. (Durham, NC) using published methodology (Evans et al., 2009). Briefly, small molecules from 5 independent livers (per genotype and ZT) were methanol extracted and analyzed by ultra-high performance liquid chromatography-tandem mass spectrometry (UPLC-MS/MS; positive mode), UPLC-MS/MS (negative mode) and gas chromatography–mass spectrometry (GC-MS). The UPLC-MS/MS platform utilized a Waters Acquity UPLC with Waters UPLC BEH C18-2.1 × 100 mm, 1.7 μm columns and a ThermoFisher LTQ mass spectrometer, which included an electrospray ionization source and a linear ion-trap mass analyzer. Samples destined for analysis by GC-MS were dried under vacuum desiccation for a minimum of 18 hr prior to being derivatized using bis(trimethylsilyl)trifluoroacetamide. Derivatized samples were separated on a 5% phenyldimethyl silicone column with helium as carrier gas and a temperature ramp from 60° to 340°C within a 17 min period. All samples were analyzed on a Thermo-Finnigan Trace DSQ fast-scanning single-quadrupole MS operated at unit mass resolving power with electron impact ionization and a 50–750 atomic mass unit scan range. Metabolites were identified by automated comparison of the ion features in the experimental samples to a reference library of chemical standard entries that included retention time, molecular weight (m/z), preferred adducts, and in-source fragments as well as associated MS spectra and curated by visual inspection for quality control using software developed at Metabolon, Inc. (Dehaven et al., 2010).

SUPPLEMENTAL REFERENCES

Dehaven, C.D., Evans, A.M., Dai, H., and Lawton, K.A. (2010). Organization of GC/MS and LC/MS metabolomics data into chemical libraries. J. Cheminform. *2*, 9.

Table 1: Gene expression overlap by ZT between SIRT6/SIRT1 WT strains

ZT	Number of genes	Percent of genes
00	24672	92
04	24820	93
08	23857	89
12	25423	95
16	23759	89
20	24151	90

Table 2: Metabolite overlap by ZT between SIRT6/SIRT1 WT strains

ZT	Number of metabolites	Percent of metabolites
00	374	99
04	376	100
08	366	97
12	373	99
16	342	91
20	360	95

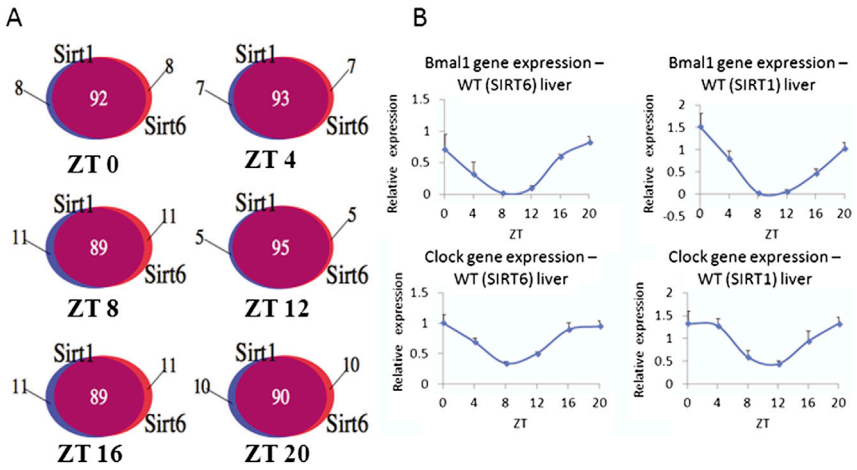

Figure S1. Comparison of WT Strains, Related to Figure 1

Differential gene and metabolite expression analyses using Cyber- T, a robust Bayesian framework that implements regularized t test. A p-value cutoff of < 0.01 was used to determine the genes/metabolites that were equally expressed by ZT in both WT strains. Tables S1 and S2 indicate percent of genes or metabolites consistently expressed in both WT strains, respectively.

(A) Overlapping genes between WT (SIRT1) and WT (SIRT6) liver strains is also shown by Venn Diagrams.

(B) Examples of gene expression profiles, as determined by real-time PCR, for *Bmal1* and *Clock* between both WT strains.

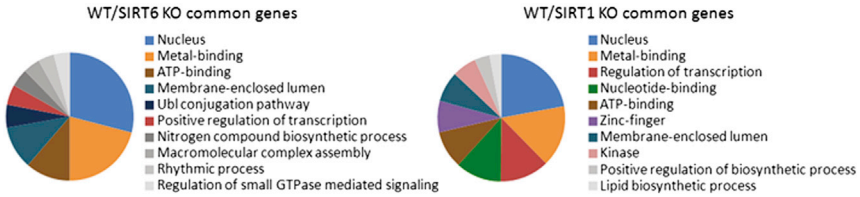

Figure S2. Biological Pathway Analysis of the SIRT6 and SIRT1 Transcriptomes, Related to Figure 1

Biological pathways using Gene Ontology (GO) terms as determined by DAVID. Common circadian genes (JTK_cycle p-value < 0.01) between WT and SIRT6 KO are shown in left panel pie chart and common oscillating genes among WT and SIRT1 KO is shown on the right side. GO terms selected include molecular function, biological process and cellular component.

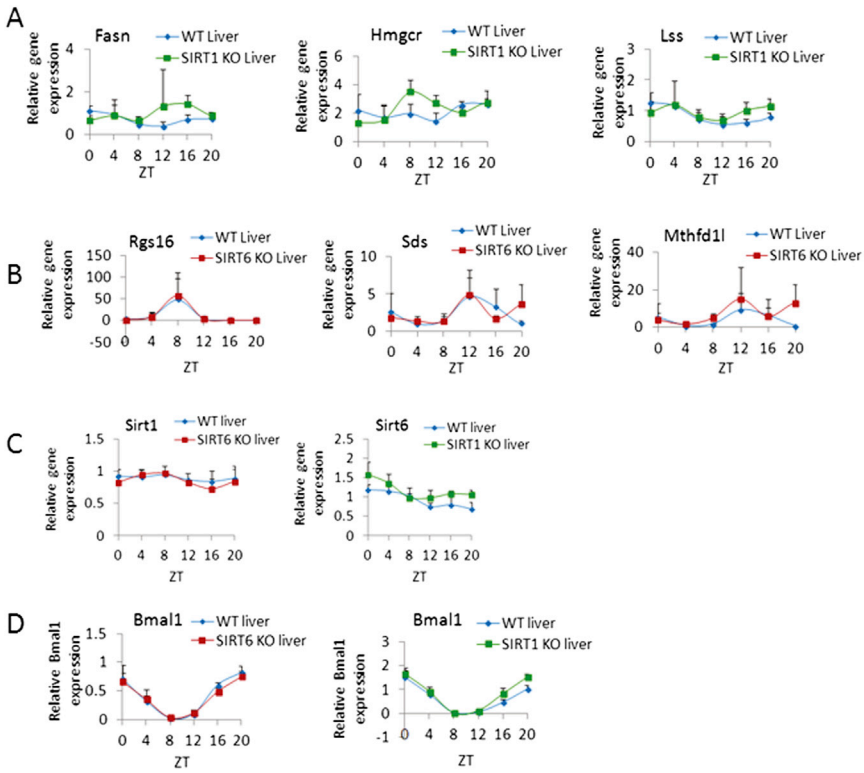

Figure S3. Gene Expression Confirming SIRT6 and SIRT1 Transcriptomes, Related to Figure 2

(A) Gene expression profiles of *Fasn*, *Hmgcr* and *Lss* genes by real-time PCR in WT/SIRT1 KO livers.

(B) Gene expression of *Rgs16*, *Sds* and *Mthfd1l* genes by real-time PCR in WT/SIRT6 KO.

(C) Gene expression profiles of *Sirt1* and *Sirt6* in SIRT6 KO and SIRT1 KO livers, respectively.

(D) Gene expression profiles for *Bmal1* in SIRT6 KO (left panel) and SIRT1 KO livers (right panel) by real-time PCR. An n = 3-5 independent livers were used per genotype and time point. Error bars indicate SEM. Significance was calculated using Student's t test and *, ** and *** indicate p-value cutoffs of 0.05, 0.01 and 0.001, respectively. Primer sequences used for gene expression analysis are listed in Table S2.

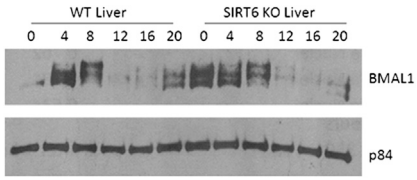

Figure S4. BMAL1 Circadian Protein Expression, Related to Figure 3

Nuclear fractions of WT and SIRT6 KO Livers were probed for BMAL1 and p84 (for nuclear loading control) over the 6 ZTs indicated.

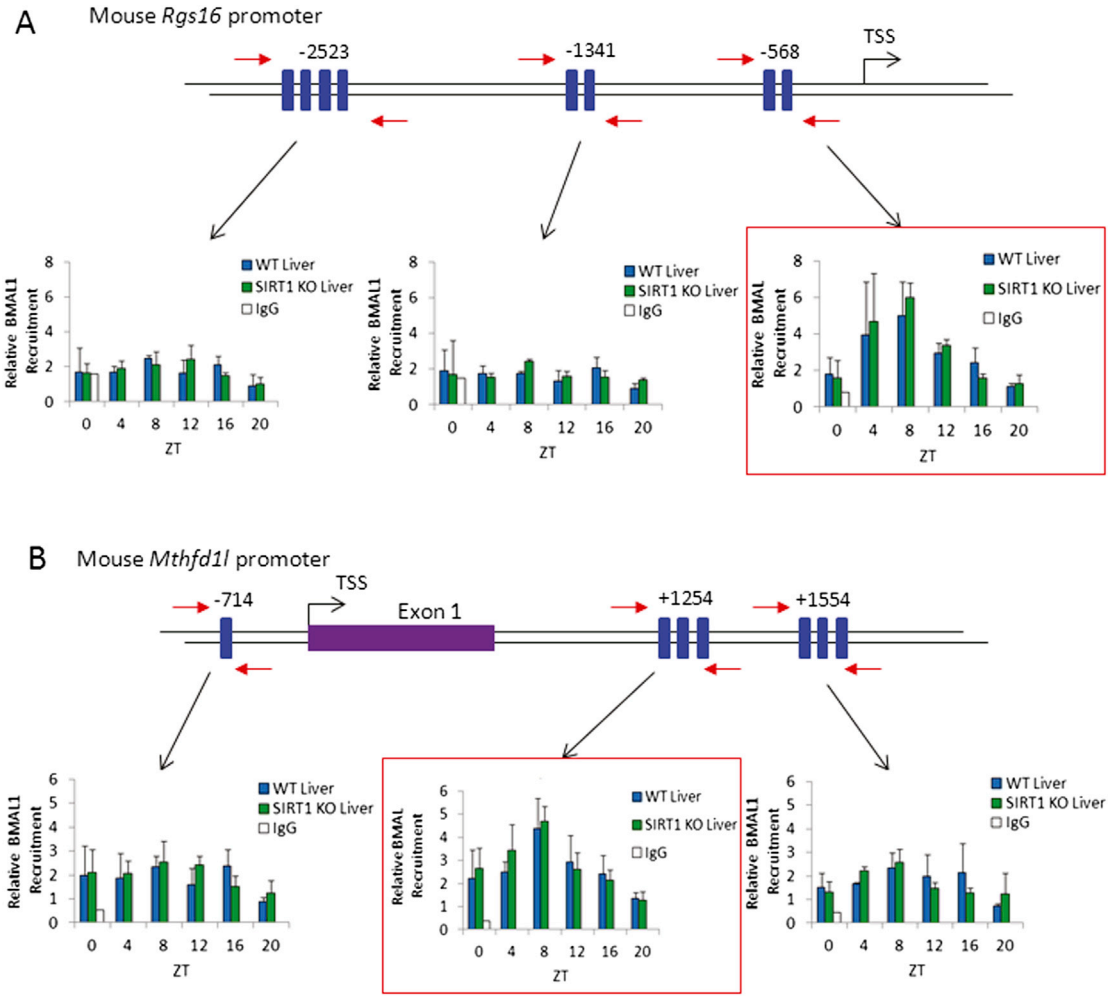

Figure S5. BMAL1 ChIP Analysis, Related to Figure 3

(A) BMAL1 recruitment to the *Rgs16* promoter by ChIP in WT and SIRT1 KO livers.

(B) BMAL1 recruitment to the *Mthfd1l* gene promoter by ChIP in WT and SIRT1 KO livers at indicated ZTs. Top panels display schematics of the promoter regions. Blue boxes illustrate locations of putative E-Boxes and red arrows indicate locations of real-time PCR primers used for ChIP. Numbers shown above E-Boxes indicate locations relative to the transcriptional start site (TSS).

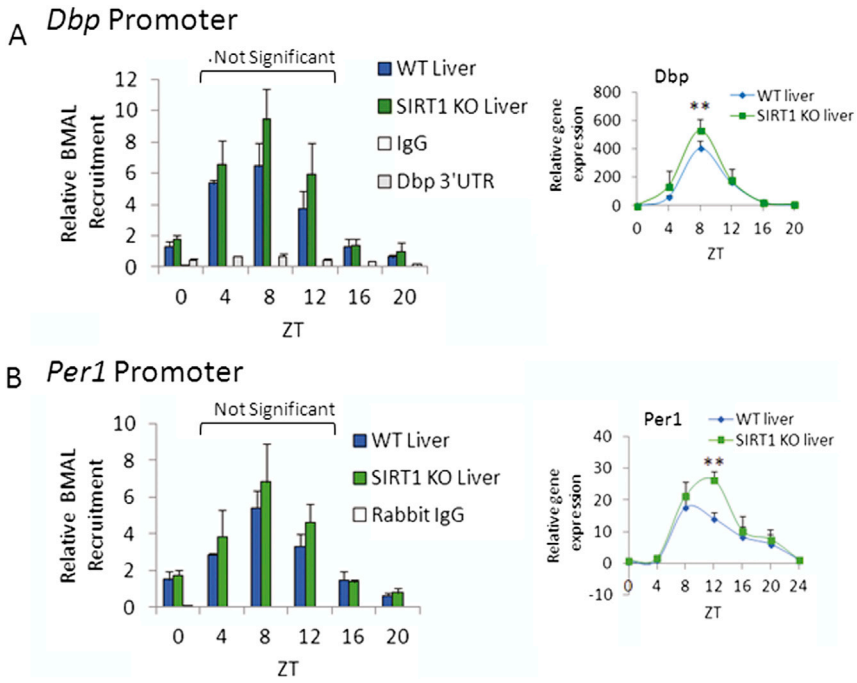

Figure S6. BMAL1 ChIP Analysis in SIRT1 Livers, Related to Figure 3

(A) BMAL1 recruitment to the *Dbp* promoter by ChIP in WT and SIRT1 KO livers shown in left panel with gene expression shown in right panel.

(B) BMAL1 recruitment to the *Per1* promoter by ChIP in WT and SIRT1 KO livers at indicated ZTs shown in left panel with gene expression shown in right panel. Error bars indicate SEM. Student's t test was used to determine that difference in BMAL recruitment at all ZTs is not significant. Difference in gene expression profiles was found to be significant at < 0.01 as indicated by **.

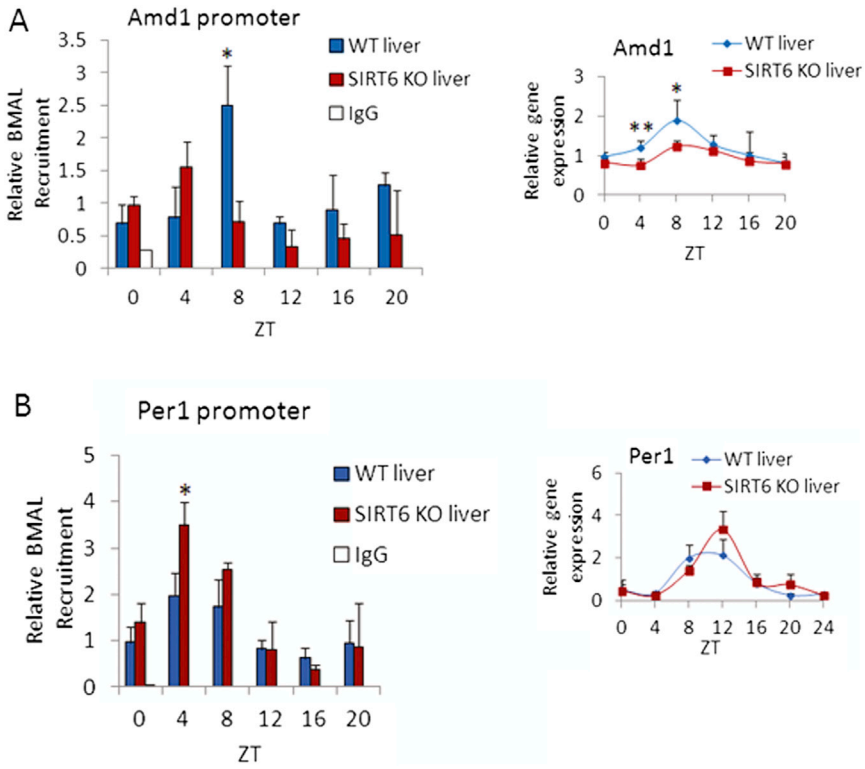

Figure S7. BMAL1 ChIP Analysis in SIRT6 Livers, Related to Figure 3

(A) BMAL1 recruitment to the *Amd1* promoter by ChIP in WT and SIRT6 KO livers shown in left panel with gene expression shown in right panel.
(B) BMAL1 recruitment to the *Per1* promoter by ChIP in WT and SIRT6 KO livers shown in left panel with gene expression shown in right panel. Error bars indicate SEM. Significance was calculated using Student's t test and * and ** indicate a p-value cutoff of < 0.05 and < 0.01, respectively.

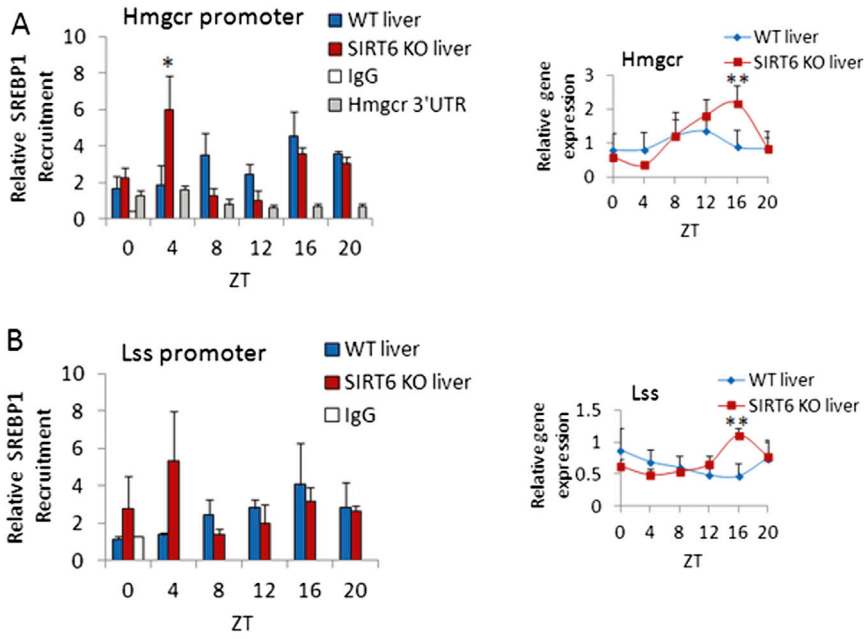

Figure S8. SREBP-1 ChIP Analysis in SIRT6 Livers, Related to Figure 5

(A) SREBP-1 recruitment to the *Hmgcr* promoter by ChIP in WT and SIRT6 KO livers.

(B) SREBP-1 recruitment to the *Lss* promoter by ChIP in WT and SIRT6 KO livers at indicated ZTs. Right panels display gene expression data for *Hmgcr* and *Lss* and left panels show ChIP data. Error bars indicate SEM. Significance was calculated using Student's t test and * and ** indicate a p-value cutoff of < 0.05 and < 0.01, respectively.